First-principles Study of Electron Transport through Atomistic Metal-Oxide-Semiconductor Structures

Xiaodong Zhang*, Leonardo Fonseca** and Alexander A. Demkov*

* Physical Science Research Laboratory, Motorola, Tempe AZ 85284
** Semiconductor Product Sector, Motorola, Mesa, AZ, 85202

ABSTRACT

We describe a theoretical scheme to combine first-principles molecular dynamics simulation and non-perturbative scattering theory for transport calculations. We compare our approach with published results for electron transport through a single Al atom. The method is then applied to the $Si/SiO_2/Si$ MOS structure, where we analyze the correspondence between the localized defect states and the leakage current. For a 1.04 nm thick MOS structure we calculate a leakage current of 33 A/cm^2, in excellent agreement with a measured value of 19 A/cm^2.

Keywords: electron transport, scattering theory, density functional, aluminum, device physics, CMOS leakage.

1 INTRODUCTION

The International Technology Road Map for Semiconductors predicts that the scaling strategy of complimentary metal-oxide-semiconductor (CMOS) devices will come to an abrupt end around the year 2012 [1]. The primary reason for this event is not lithography scaling problems as was previously thought, but rather meeting an acceptable leakage current through the silicon dioxide layer with a thickness below 2 nm [2]. The end of SiO_2 as a gate insulator has spurred an active search for an alternative gate dielectric. However, finding such a material has proven to be far from trivial.

Because the scaling laws of the semiconductor device design are pushing the technology to atomic scale ultrathin SiO_2 layers [2], the low bias leakage current may be affected by atomic details of the dioxide layer's structure. For ultra-thin SiO_2 barriers where the atomic structure of the interface is important, traditional approaches, such as the WKB approximation, to tunneling across an empirically defined potential barrier are not appropriate. Instead we need a theoretical approach that not only correctly predicts the bonding patterns at the interface, but also describes how different chemical environments affect the leakage current. Density functional (DFT) theory provides the information on the chemical bonding, structure, band offsets, and stability of the Si/dielectric interface.

A diverse array of DFT-based techniques has been developed for dealing with the electron transport in molecular systems including the time-dependent solution of the Schrödinger equation [3], self-consistent [4] and not self-consistent [5] time-independent non-equilibrium Green's functions, non-perturbative solutions of the open boundary Schrödinger equation [6], transfer matrix techniques [7], as well as indirect estimates of transport properties from the electronic band structure of an isolated molecule [8].

In this paper, we describe the use of the DFT Hamiltonian within a non-perturbative scattering theory framework for transport calculations. We first consider a single Al atom weakly coupled to Al leads, and show that this theory can identify the contributions of individual atomic states. We also investigate the strongly coupled case and compare our findings with the published data. We then apply our approach to the electron transport across a $Si/SiO_2/Si$ model MOS structure. The calculated leakage current for a simulated 1.04 nm MOS structure agrees with recent experimental data. We show how the atomic structure and chemistry of the MOS structure are reflected in its transport properties that can be accessed experimentally.

2 THEORY

The total transmitted current flowing thorough an atomic structure is given by

$$I = \frac{8\pi^2 e}{h}\int_{-\infty}^{+\infty} dE \sum_{l,r} |T_{lr}(E)|^2 \times \quad (1)$$

$$[f(E-\mu_l) - f(E-\mu_r)]\delta(E-E_l)\delta(E-E_r),$$

where μ_l and μ_r refer to the electrochemical potential of the left and right gate electrodes, respectively, and a multiplicative factor of two has been included to account for spin degeneracy. The transmission matrix element T_{lr} is the matrix element of the scattering operator $\hat{T}$ which is given by the Lippmann-Schwinger equation,

$$\hat{T} = \hat{V} + \hat{V}\hat{G}\hat{V} \quad (2)$$

Here we do not make any approximations, and $\hat{T}$ is accurate to all orders.

In the limit of low temperature, the Fermi functions can be approximated by step functions resulting in the final expression for the total current:

$$I = \frac{2e}{h}\int_{\mu_l}^{\mu_r} dET(E) \quad (3)$$

where the transmission function T(E) is given by

$$T(E) = 4\pi^2 \sum_{lr} | T_{lr}(E) |^2 \delta(E - E_l)\delta(E - E_r) \quad (4)$$

Plugging Eq. 2 into Eq. 4, we directly obtain [9]:

$$T(E) = Tr[\hat{\Gamma}_r \hat{G}_d \hat{\Gamma}_l \hat{G}_d], \quad (5)$$

where the indices *l,r,d* stand for the left, right, and "defect" (*i.e.* the scattering region) portions of the modeled system, respectively. We shall employ a local orbital basis, therefore in the Löwdin representation the "defect"-lead coupling matrix has a finite range, and only the "defect" portion of the Green's function:

$$\hat{G}_d = \frac{I}{E - \hat{H}_d^0 - \hat{\Sigma}_l - \hat{\Sigma}_r} \quad (6)$$

enters the expression for the transmission function. $\hat{\Gamma}_i$ and $\hat{\Sigma}_i$ (i=l,r) are given by

$$\hat{\Gamma}_i = \sum_i \hat{V}_{di} | i\rangle\langle i | \delta(E - E_i)\hat{V}_{di}^{+} = \hat{V}_{di}\hat{\Delta}_i\hat{V}_{di}^{+}$$
$$\hat{\Sigma}_i = \hat{V}_{di}^{+}\hat{G}_i^0\hat{V}_{di}, \quad (7)$$

and describe the leads, and the "defect" region's coupling to them. Note that the self-energy **Σ** is a complex operator, and reflects the use of the open boundary conditions. The effects of the leads density of states are automatically included *via* the spectral density operator, given by the following identity:

$$\hat{\Delta}_i = \delta(E - \hat{H}_i) = \sum_i \delta(E - E_i) | i\rangle\langle i |. \quad (8)$$

Due to the sparse nature of the Hamiltonian, only surface parts of the semi-infinite Green's functions of the leads are required and can be calculated by the block-recursion. It should be emphasized that Eq. 5 comes directly from the Lippmann-Schwinger equation, and is therefore exact.

In the presence of an applied external bias V, the transmission function *T(E)* depends on *V*, namely *T(E)* is written as *T(E,V)*. In this work we adopt the rigid band approximation:

$$T(E,V) = T(E + \eta V), \quad (9)$$

so that the current can be written as:

$$\begin{aligned} I &= \int T(E,V)(f(E - E_f - V) - f(E - E_f))dE \\ &= \int_{E_f}^{E_f+V} T(E,V) \\ &= \int_{E_f-\eta V}^{E_f+(1-\eta)V} T(E)dE \end{aligned} \quad (10)$$

where η is the voltage division factor. In this work, we follow Datta *et al.*, and η is taken as 0.5.

3 RESULTS

We apply our method to two very distinct systems: the single-atom Al bridge connecting two semi-infinite Al slabs, and the $Si/SiO_2/Si$ barrier. The first problem has been well studied theoretically in recent years by several groups and is a good test case for models [6,10]. We find that our approach works very well on this system. The second problem is motivated by the small dimensions of oxide barriers used in CMOS devices currently under development [11,12]. Our goal is to determine how the individual atomic states at the Si-SiO_2 interface affect tunneling.

In this work all the electronic Hamiltonians are generated using the local atomic orbital first principles density functional package FIREBALL. This package has been successfully used to study various materials problems. For a recent review of this technique the reader is referred to reference [13]. As shown later, the combination of a local orbital basis with the Green's function technique results in a very flexible and efficient scheme to describe transport properties at the atomic level.

3.1 Transmission through single Al atoms

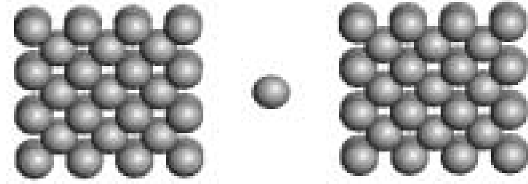

Fig.1:Schematic representation of the structure investigated

We considered a single Al atom between two Al electrodes. The model system is described by a supercell built using a (2x2) (110) Al surface cell that is 14 Al layers deep. The cell dimensions are 8.1x5.73x20.3 $Å^3$. Three Al atoms are deleted in the middle plane normal to the *c* axis of the supercell. The remaining one atom bridges the left and right sides of the cell, and is the main channel for electrons flowing between them. However, because the two sides are so close to each other, we also calculate the current for a structure containing no bridging atom, but rather a 2.8 Å gap, in order to subtract out the current created by electrons tunneling between the slabs without going through the atomic bridge. We use periodic boundary conditions in two lateral directions, and lateral lattice constants (a=8.1 Å, b=5.73 Å) that are just big enough to avoid a sizable interaction between the atomic bridge and its periodic image. Four layers of bulk Al atoms in the lead regions were used to perform the block-recursion required to generate the Green's function of the semi-infinite leads [9].

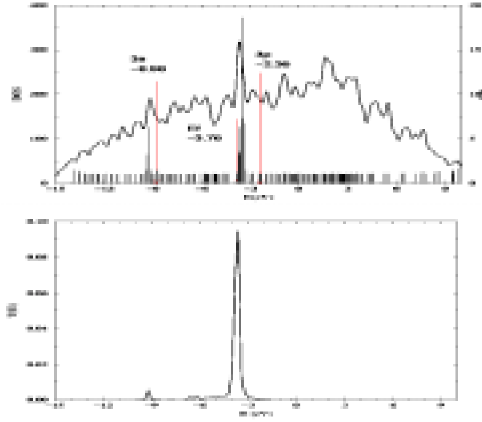

Fig.2: Top: Weak coupling limit. The black solid line shows the density of states and vertical lines give the inverse participation ratio. The tall/short red lines indicate the eigen energies of the isolated Al atom and the system's Fermi energy, respectively. Bottom: the transmission function through the Al bridge atom in the weak-coupling limit.

The distance between the Al atom and the electrodes was varied to distinguish two important scenarios: the weak and strong coupling. First, we discuss the weak coupling case. The DFT calculation of an isolated single Al atom predicts the location of the 3s and 3p levels at –8.98 eV and –2.36 eV, respectively. With the single Al atom separated from each electrode by 5 Å (see Fig. 1), a calculation of the inverse participation ratio (IPR) shows that there are two strongly localized states corresponding to the atomic states of the isolated Al atom (the small energy shift is due to the coupling between the bridge atom and electrodes). Indeed, the contributions of these two states are also clear in the density of states (DOS) of this system (the broadening of the atomic levels is again due to the coupling with electrodes). Figure 2 (the lower panel) clearly shows the propagation through resonant states belonging to a weakly bound atom: only electrons with energy matching the quasi-atomic orbitals of the bridge atom flow through this structure.

The upper panel of Fig.3 shows the DOS and IPR of a single Al atom sandwiched between two Al electrodes in the strong coupling limit, where the bridge atom/electrode separation of 1.4 Å is close to the experimental interlayer separation in bulk Al along the (110) direction. The red/black line shows the projected DOS and IPR at the bridge/bulk Al atom, respectively. Notice, that the electronic structure of the bridge atom is not much different from the bulk Al atoms surrounding it. All the states are well delocalized due to the strong coupling between all the Al atoms. The transmission shown in the bottom panel of Fig.3 is the difference between the transmission when the single Al atom is present between the electrodes and the transmission without the bridge atom. This result is in agreement with the calculation by Cuevas et al. [10].

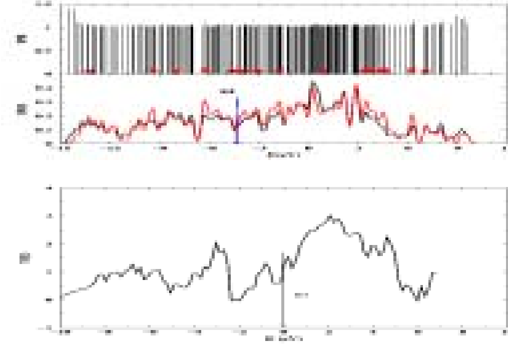

Fig.3: Strong coupling limit. Top: density of states and inverse participation ratio. Bottom: transmission function.

3.2 Atomistic transport through an MOS structure

To accurately describe the transport through MOS structures we generated a model of the Si/SiO_2 interface by the "direct oxidation" method [11]. The model consists of a silicon slab with an oxide layer "grown" on top of it in a quantum molecular dynamics (QMD) simulation. The Si layers are separated from the stoichiometric oxide by approximately 4 Å of suboxide. Then, in the simplest case, a mirror image of the cell is generated, and the two are fused together. That procedure results in a $Si/SiO_x/SiO_2/SiO_x/Si$ structure. Some special care needs to be taken of the SiO_2 bonding pattern in the plane of contact. Mixing and matching the initial Si/SiO_2 structures, both symmetric and asymmetric MOS models could be built. The structure then is annealed in a high-temperature QMD run followed by a quench to a local energy minimum. MOS model structures thus generated are used as scattering regions or "defects". In particular we consider here tunneling through such a defect with the oxide thickness of 10.2 Å and a 5.43 Å x 5.43 Å cross-section. The interface region of the relaxed simulated MOS capacitor is shown in Fig. [4]. There are no dangling bonds in the model. Once we have the defect model, two perfect Si regions with the same cross section as the defect, representing the leads, are considered attached to both sides of the defect. Thus the total length of the system is taken to infinity. The right Si region represents the channel, and the left region a grain of poly-Si (gate electrode).

Our goal is to investigate how the atomic structure of the interface translates into transport characteristics. There are three distinct types of possible defects in our structures: suboxide SiO_x regions where the oxidation state of Si gradually changes from 0 to +4; oxidation induced strain; and interfacial defects such as dangling bonds. As seen in Fig.4, the defect labeled 2 is the suboxide Si, while the defect labeled 1 is the oxidation induced strain defect in

which one Si-Si bond is elongated. The simulated structure does not have dangling bonds as evidenced by the clean gap in the corresponding DOS (Fig. 5).

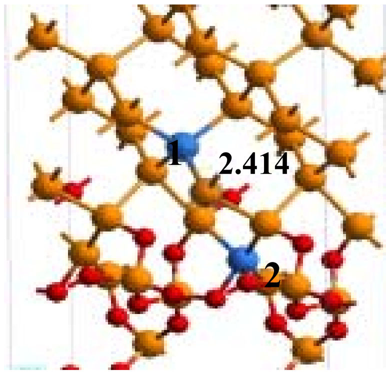

Fig.4: The interface region of the simulated MOS structure. Blue color indicates defects at the interface.

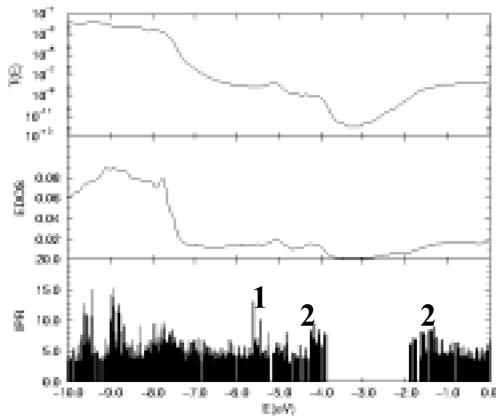

Fig.5: The transmission function, local density of states and inverse participation ratio of the simulated MOS structure.

In the suboxide layer, a Si atom bonded to three Si neighbors and one oxygen produces a localized state in the valence band at -4.2 eV as well as a state at -1.6 eV in the conduction band (label 2 in Fig.5). The “suboxide'” states dominate the valence band edge. Deeper into the band, at an energy of -5.6 eV (label 1), we see localized states induced purely by the oxidation strain causing a distortion of the Si bonding near the interface. The localized states are clearly visible in the IPR plot and are directly related to corresponding peaks in the transmission function. If somehow these defects could be eliminated, the resulting structure might display a reduced leakage. However, our recent studies show that it is very difficult, if not impossible, to build a perfect interface without the suboxide. Even the Si/SiO_2 model with no nominal interface layer recently proposed by Buczkko *et al*. [14] contains about 4 Å sub-oxide [9].

The leakage current for MOS structures with the oxide thickness ranging from 4 Å to 32 Å have been recently measured at Bell Labs [15]. They have found leakage current densities of 19 A/cm^2 and 10^{-3} A/cm^2 for a 35 nm gate length transistor with oxide thickness of 10.2 Å and 19.0 Å, respectively. Using the crossectional area of 29.5 Å^2 and the current of 9.84 x 10^{-2} pA at a bias of 1 V our theory predicts a current density of 33.2 A/cm^2 for a 10.2 Å barrier structure (19.0 Å total oxide thickness), in remarkable agreement with experiment. Here, we would like to emphasize that a 4 Å sub-oxide is almost intrinsic at the Si/SiO_2 interface, so the width of the tunneling barrier should be reduced by the thickness of the sub-oxide. This is one of the reasons for the failure of the phenomenological barrier picture to estimate leakage current through very thin barriers [12].

4 CONCLUSION

Using a combination of density functional quantum molecular dynamics and ballistic transport theory we generated ultra-thin MOS structures and investigated the leakage current through them. Our technique provides a direct correspondence between features in the I-V characteristic and the microscopic nature of the device

REFERENCES

[1] 1999 International Technology Road Map for Semiconductors, San Jose (1999).

[2] D. A. Muller *et al*., Nature,**399**,758 (1999).

[3] John K. Tomfohr and Otto F. Sankey, Phys. Stat. Sol. (b) **226**, 115, (2001).

[4] M. Brandbyge et al. Phys. Rev. **B 60**, 17064 (1999).

[5] M. P. Samanta, W. Tian, and S. Datta, Phys. Rev. **B 53**, R7626 (1996).

[6] N. D. Lang, Phys. Rev. **B 52**, 5335 (1995).

[7] E. G. Emberly and G. Kirczenow, Phys. Rev. B **58**, 10911 (1998).

[8] J. M. Seminario, Angelica G. Zacarias, and James M. Tour, J. Am. Chem. Soc. **122**, 3015 (2000).

[9] Xiaodong Zhang, L.R.C. Fonseca, Heather Loechelt, and A. A. Demkov, unpublished.

[10] J. Cuevas *et al*., Phys. Rev. Lett. **80**, 1066 (1998).

[11] A. A. Demkov and O. F. Sankey, Phys. Rev. Lett. **83**, 2038 (1999).

[12] A. A. Demkov, Xiaodong Zhang, and D. A. Drabold, Phys. Rev. **B 64**, 125306 (2001).

[13] O. F. Sankey *et al*., Int. Journ. of Quant. Chem. **69**, 327 (1998).

[14] R. Buczko, S. J. Pennycook and S. T. Pantelides, Phys. Rev. Lett. **84**, 943 (2000).

[15] M. L. Green *et al.*, Microelectronic Engineering, **48**, 25-30, (1999).